Applying Synchronous Condenser for Damping Provision in Converter-dominated Power System

Ha Thi Nguyen, Guangya Yang, Arne Hejde Nielsen, Peter Højgaard Jensen, and Bikash Pal

***Abstract*—The dynamic characteristics of converter-dominated systems are governed by controlling power converters and the interactions between converter systems and conventional alternators. Frequency oscillations can appear under dynamic operation conditions caused by the phase-locked loop dynamics and interactions among the converter control systems. The oscillations may be poorly damped, which can result in reduced power generation, longer settling time, or disconnections of sensitive components. It is foreseeable that damping services will be critical for power grid stabilization in the future with high penetration of renewable generation. In this work, synchronous condensers (SCs) are evaluated and applied to provide damping services to the power grid under post-event conditions. An innovative supplementary controller for the automatic voltage regulator of SCs is proposed to improve the frequency stabilization in a converter-dominated system after disturbances. Using local and remote measurements, SCs are able to modulate the reactive power output and hence, the terminal bus voltage, which further impacts the power flow in the system; therefore, damping can be provided to the frequency oscillations. The control is implemented on an industrial-level hardware platform, and the performance is verified by the hardware-in-the-loop simulation.**

***Index Terms*—Power oscillation, Prony analysis, low-inertia system, supplementary controller, synchronous condenser (SC).**

I. Introduction

SYNCHRONOUS condensers (SCs) have a long historical use in power systems for reactive power compensation. SCs have been applied to many power grids in the world for dynamic voltage regulation and short-circuit current support [1]-[9].

The increasing penetration of renewable energy sources (RESs) into power systems has introduced many challenges in securing a stable network operation and has forced power systems to operate under low-inertia conditions. The systems based on converter-interfaced RESs do not have the stronghold as conventional systems due to the lack of synchronous machines in operation. In such a system, the internal dynamics against an external disturbance are highly dependent on the control of the main converter stations and their interactions among themselves as well as with the synchronous units. SCs have been proven as an effective solution for supporting the system dynamic performance and renewable interconnection in low-inertia systems. SCs providing inertial and frequency responses in renewable-based systems are investigated in [10]-[13].

For the converters, the frequency and power are coupled through their control systems. For the systems, this artificial coupling can affect the frequency as a global parameter for power regulation due to the heterogeneous design and response of the measurement and control systems of the converters. When the number of the converters increases in a system, the locality of frequency increases, which increases the heterogeneity of the entire network. Hence, faster frequency dynamics with unexpected power oscillations may occur at the system level under different operation conditions and various generator combinations after an external disturbance.

A frequency response with faster dynamics and an undesirable oscillation during a generation loss disturbance is experienced in the simulated Great Britain power system due to inertia reduction [14]. The impact of wind power penetration on the low-frequency oscillation modes of the IEEE 39-bus New England power system is investigated in [15]. The oscillation frequency is dependent on the inherent inertia of the involved network (can be a sub-network) as well as the bandwidth of the measurement and control systems of the converters within the network. Traditional power system stabilizers (PSSs) do not work well for SCs and will not be suitable for renewable-based systems where synchronous generators will be gradually phased out.

To help improve the frequency dynamic and the damping of the oscillations at the system level, this study exploits the controllability of SCs. As the SC itself does not control active power, the control effect on system power and frequency oscillations will be provided through its reactive power channel via its excitation control. SCs can provide damping torque via its fast excitation control, which has been theoretically proven by the small-signal analysis [16].

To provide damping in frequency for converter-dominated systems by using SCs, this study proposes a design principle

Manuscript received: April 2, 2020; accepted: August 19, 2020. Date of Cross-Check: August 19, 2020. Date of online publication: September 11, 2020.

This work was supported by Synchronous Condenser Application (SCAPP) project funded by ForskEL program (No. 12196) administrated by Energinet.dk.

H. T. Nguyen and A. H. Nielsen are with the Department of Electrical Engineering, Danmarks Tekniske Universitet, Roskilde, Denmark (e-mail: thangu@elektro.dtu.dk; ahn@elektro.dtu.dk).

G. Yang (corresponding author) is with the Electrical Engineering, Technical University of Denmark, Lyngby, Denmark (e-mail: gyy@elektro.dtu.dk).

P. H. Jensen is with Siemens AG Sektor Energie, Ballerup, Denmark (e-mail: peter_hoejgaard.jensen@siemens.com).

B. Pal is with the Department of Electrical and Electronic Engineering, Imperial College London, London, UK (e-mail: b.pal@imperial.ac.uk).

DOI: 10.35833/MPCE.2020.000207

of a power oscillation damping (POD) controller as a supplementary controller for SCs, where reactive power is used to modulate the active power flow of the main flow paths in the system through node voltage regulation. In this way, active power oscillations after the disturbance can be damped quicker, and the system can regain a stable frequency sooner after a major frequency disturbance. The design uses both local and remote measurements from the systems, where in the proposed controller, the measurements of local frequency and a remote tie-line flow are used as inputs, while the measurement of SC reactive power is used as the output. By modulating the SC bus terminal voltage in terms of the magnitude and phase, the active power of transmission lines and loads in the system can be affected on a global scale, which helps damp the oscillations and enhance the frequency stability on the frequency nadir and settling time.

This study is purely based on electromagnetic transient simulation (EMT) in real-time digital simulator (RTDS). A parameter optimization based on software-in-the-loop (SiL) linking RTDS and MATLAB through object linking and embedding for process control (OPC) communication is implemented [17]. The Prony technique is applied to extract the dominant oscillation frequency and damping ratio from the system frequency measurement. The near-optimal or optimal parameter set of the POD controller is determined by a gradient-free algorithm to maximize the damping effect. To validate the effectiveness of the proposed POD controller, a prospective future western Danish power system (denoted as DK1) supplied by RESs and multiple interconnections with neighboring countries is used. Comparative results show that the POD controller can provide enhancement in the system in terms of oscillation damping and frequency stability.

The remainder of this paper is organized as follows. The proposed POD controller is clarified in Section II, which explains the impact of SC on the improvement of the POD and frequency stability during disturbances via its reactive power control channel. Section III describes the communication system setup of the control parameterization by RTDS, MATLAB, and OPC. Based on the proposed POD controller, the prospective future DK1 is used to test the low-inertia system of the POD controller in Section IV. Finally, conclusions are drawn in Section V.

II. Design Methodology and Proposed POD Controller

Power oscillations in a converter-dominated system can take place between the subnetworks, where a cluster of dynamic components, including line-commutated converter (LCC) based high-voltage direct current (HVDC) links, synchronous and non-synchronous generators, and loads, are located in a vicinity where similar local information is presented to their control systems. A subnetwork may represent a center of inertia, where the components in a subnetwork can oscillate against one or several other subnetworks in the system during a disturbance. This phenomenon is considered as inter-area oscillations, where the characteristics are governed by synchronous machines. However, with the increasing amount of power converters in the system, the control system of power converters starts to play a major role in the oscillation analysis. A number of field events have been reported in recent years.

A. Design Methodology

The oscillations in a system can be suppressed by controlling the critical flow paths in a network. This can be achieved by controlling the active or reactive power of the controllable units in the system, provided a designated control system can handle the expected oscillatory frequencies. To effectively achieve the damping effect, using the measurements of line flows might be considered as immediate inputs for a controller. SCs can only provide volt/var control to a system; however, volt/var control can impact the system power flow in a number of ways, as described below.

The mathematical formula of the transferred active power on a simplified transmission line can be expressed as:

$$P = \frac{V_1 V_2}{X} \sin \delta \tag{1}$$

where V_1 and V_2 are the line-to-line voltages of the two end sides of the transmission line; δ is the angle of V_1 with respect to V_2; and X is the reactance of the transmission line.

The active power of a load expressed in a voltage- and frequency-dependent load model [18] is expressed as:

$$P_{Load} = P_0 (1 + k_{Pf} \Delta f) \left(p_p + p_c \frac{V}{V_0} + p_z \left(\frac{V}{V_0} \right)^2 \right) \tag{2}$$

where P_0 is the rated active power of the load; V_0 and V are the nominal and actual voltage magnitudes at the load bus, respectively; Δf is the frequency deviation; k_{Pf} is the frequency characteristic coefficient; and p_p, p_c, and p_z are the portions of the total load proportional to constant active power load, constant current load, and constant impedance load, respectively.

The active power of the LCC-HVDC link at the rectifier is expressed as:

$$P_{HVDC} = 1.654 V_m I_d \cos \alpha \tag{3}$$

where V_m is the peak line-to-line voltage of the AC terminal; I_d is the DC current of the LCC-HVDC link; and α is the firing angle of the rectifier.

The basic control principle of the LCC-HVDC link is that the rectifier controls the DC current and the α limit, whereas the inverter is responsible for controlling the extinction angle constantly to keep the transferred power tracking the set point.

According to (1)-(3), the active power on the transmission lines, LCC-HVDC links, and loads can be manipulated by the AC terminal voltage, which can be controlled via the excitation of SCs with a supplementary POD controller. The principle of the proposed POD controller is to control the terminal voltage in terms of the magnitude and phase via the excitation of SCs, which in turn adjusts the active power of the loads and LCC-HVDC links, and the power transferred on the transmission line connected directly to the SC terminal. Consequently, it helps damp the oscillation in voltage, power, and frequency.

B. POD Controller

A POD controller incorporating SCs adapting to modern system is developed. By regulating the terminal voltage through reactive power modulation, the POD controller controls the active power transferred on the transmission lines, LCC-HVDC links, and loads to damp the power oscillation and improve the frequency stability.

The lead-lag control structure is still preferred owing to a better tradeoff between the static accuracy, system stability, and insensibility to disturbances in the frequency domain [19]. Low-frequency oscillation can be efficiently damped by the proper selection of lead-lag block parameters.

In the literature, many valuable input signals of the POD controller are suggested, including the rotor speed deviation, frequency, electric power, and acceleration power [20] - [22]. Notably, the frequency behavior represents the active power oscillation or imbalance; therefore, it is selected as an input to damp the power oscillation. Furthermore, because of the locality of the frequency in a low-inertia system, it is essential to select a signal from the central path of the oscillation as one of the inputs; the measured tie-line flow between the Danish and German systems is selected in this case. In implementation, this measurement is best taken by the synchrophasor measurement units to maintain the time synchronization with the local measurements.

Figure 1 shows the structure of the proposed POD controller. The POD controller takes a local frequency measurement f and active power on a tie line $\Delta P_{tieline}$ as input signals to create a POD output V_{POD}, which is then added to the automatic voltage regulator (AVR) of the SC. This output regulates the excitation field current to control the terminal voltage, which therefore changes the active power on the tie line, LCC-HVDC links, and voltage-dependent loads to enhance the power oscillation and frequency deviation during disturbances.

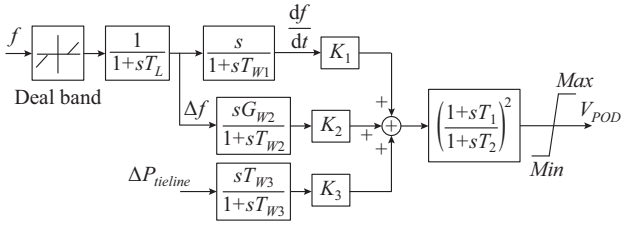

Fig. 1. Structure of proposed POD controller.

To begin with the first input signal f, a dead band is applied to eliminate small frequency changes that may result in an unexpected contribution of POD under steady-state conditions. A low-pass filter $1/(1+sT_L)$ filters the measurement noise that can cause the control function to be poor. There are two control signals created by the frequency measurement. The first one, with a smaller time constant T_{W1}, works similar to a differentiation to capture the rate of change of frequency (ROCOF) during frequency excursions. The second one, with a larger time constant T_{W2}, catches the frequency deviation to generate a signal with a longer response time; G_{W2} is a gain that is equal to 1 in this case. The second input signal $\Delta P_{tieline}$ first moves through a filter $sT_{W3}/(1+sT_{W3})$, which allows the desired frequency oscillation mode (inter-area oscillation around 0.1 Hz to 1.5 Hz) to pass and optimizes the compensation at a low-frequency range (normally less than 0.5 Hz).

The magnitude and phase shift of the output are adjusted through control gains (K_1, K_2, and K_3) and the lead/lag time constants (T_1 and T_2) to compensate for the system oscillation. They are optimized by the objective function of genetic algorithms (GAs). The GA objective is to maximize the damping ratio of the dominant oscillation mode of the system frequency.

A limiter is a crucial part of each controller that hedges control participation with uncertainty. This limiter is more critical when the SC is connected to the same bus with voltage-sensitive components such as photovoltaic (PV) sources or wind power plants, which have strict fault ride-through requirements and voltage-based protection settings. These limitation values may change from site to site depending on the grid codes.

III. Control Tuning Procedures

The tuning procedure is based on the EMT simulation of a detailed power grid model, where on top of the simulation model, a non-linear optimization procedure is added to optimize the controller parameters with respect to system performance. This is by far the most suitable procedure with respect to EMT simulation, as conventional analytical eigenvalue analysis is exclusively used for the representation of the stability analysis function of the system, where the dynamics inside the converter control are ignored owing to the mismatch between the operation time scales.

A prospective power system run on the RTDS platform is driven by a MATLAB script for system startup and disturbance simulations, as shown in Fig. 2. The data of the system are collected by an OPC server and sent directly to the MATLAB workspace. In MATLAB, the signal is first processed to separate the oscillation component by a polynomial function. The oscillation component is then analyzed by the Prony technique for extracting the frequency and damping ratio of the dominant oscillation mode. The damping ratio is maximized by a GA objective function to determine the optimal parameters of the POD. GA is a global heuristics parameter search technique based on genetic operators to find the optimal or near-optimal solutions for each specific problem [23], [24]. Unlike traditional optimization approaches that require one starting point, GA uses a set of points (chromosomes) as the initial condition, and each chromosome is evaluated for its performance according to the objective function that characterizes the problem to be solved and defined by the designers. Subsequently, these parameters are updated on the RTDS model for further verification. These steps are iterative by a closed loop and run in real time with the RTDS, OPC, and MATLAB communications. The closed loop continues until the objective function satisfies the damping ratio maximization of the dominant oscillation mode constraint to determine the optimal values of POD parameters.

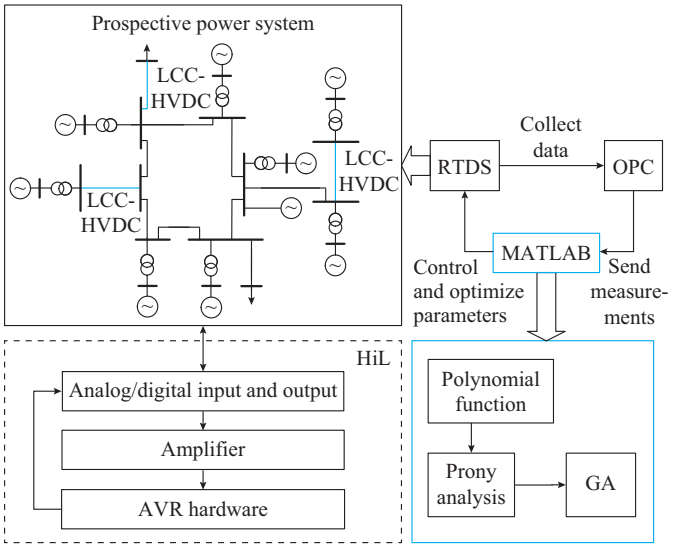

Fig. 2. System arrangement of hardware-in-the-loop (HiL) and SiL simulations.

A. Prony Analysis

Prony analysis is a least-square approximation technique for fitting a linear sum of exponential terms to a measured signal. A brief overview of this technique is given in [25]. An important feature of this technique is that it directly determines the frequency, damping ratio, energy, and relative phase of the modal components present in a given measurement signal by an extended Fourier analysis [26]. The ability to extract such information from transient signal simulations would overcome the computing burden of the linear model for large-scale systems.

Consider a generally continuous signal $y(n)$ that is modeled as:

$$y(n)=\sum_{i=1}^{p} b_i z_i^n=\sum_{i=1}^{p} A_i \mathrm{e}^{\mathrm{j}\theta_i}\mathrm{e}^{(\alpha_i+\mathrm{j}2\pi f_i)n\Delta t} \tag{4}$$

where $b_i=A_i\mathrm{e}^{\mathrm{j}\theta_i}$; $z_i=\mathrm{e}^{(\alpha_i+\mathrm{j}2\pi f_i)n\Delta t}$; $n=0,1,...,N-1$, and N is the sampling number; Δt is the time interval of sampling; p is the order of the Prony mode; A_i and θ_i are the amplitude and inception phase angle of the i^{th} oscillation mode, respectively; and f_i and α_i are the frequency and damping ratio of the i^{th} oscillation mode, respectively.

Overall, Prony analysis can be summarized into three steps:

Steps 1: construct a linear prediction model from the measured data and solve it.

Steps 2: compute the discrete-time poles of the characteristic polynomial equation generated by the linear model, which in turn results in the eigenvalues.

Steps 3: extract the damping ratios, oscillation frequencies, and related parameters from these eigenvalues.

Before determining the information of the measured data, a signal processing step is implemented to remove the fundamental frequency. This step separates the oscillatory component for the Prony analysis conduction. The Prony analysis obtains many oscillation modes, including dominant oscillation modes and noise oscillation modes. This observation results from the mixing noise and trend in the measurement, which cannot be eliminated completely in the signal processing step.

The dominant oscillation mode is recognized by the energy analysis approach, which evaluates the contribution of each oscillation mode and is expressed as:

$$E_i=\sum_{n=0}^{N-1}(R_i z_i^n)^2 \tag{5}$$

where E_i, R_i, and z_i are the energy, amplitude, and pole of the i^{th} oscillation mode, respectively, and $i=1,2,...,p$. The dominant oscillation mode is the largest energy contribution to the oscillation.

B. Overall Fitting Procedure

In this study, five parameters (T_1, T_2, K_1, K_2, and K_3) of the proposed POD controller are optimized by the objective function of a damping ratio maximization through a gradient free solver, which is a GA in this case. The main control design goal is to maximize the damping ratio of the system oscillation mode.

$$f(x)=\max\left\{\xi=-\frac{\alpha}{\sqrt{\alpha^2+\beta^2}}\right\} \tag{6}$$

s.t.

$$T_{i,\min}\le T_i\le T_{i,\max}\quad i=1,2 \tag{7}$$

$$K_{j,\min}\le K_j\le K_{j,\max}\quad j=1,2,3 \tag{8}$$

where α and β are the real and imaginary parts of the dominant oscillation mode, respectively; ξ is the damping ratio of the dominant oscillation mode; and the subscripts min and max represent the minimum and maximum values of corresponding variables, respectively. The optimization determines the variable x (T_1, T_2, K_1, K_2, or K_3) based on the boundary settings to maximize ξ. Table I lists the boundary settings of the proposed POD controller, where *Max* and *Min* are the maximum and minimum values of the limiter.

TABLE I
BOUNDARY SETTINGS OF PROPOSED POD CONTROLLER

$T_{1,\min}$	$T_{1,\max}$	$T_{2,\min}$	$T_{2,\max}$	$K_{1,\min}$	$K_{1,\max}$
0.01	10	0.01	10	0.5	50
$K_{2,\min}$	$K_{2,\max}$	$K_{3,\min}$	$K_{3,\max}$	*Min*	*Max*
0.5	12	0.05	2	–0.13	0.13

IV. Case Study

The case study is based on an observed damped oscillation after major frequency disturbances, which causes a long settling time in frequency after disturbances. The system is a modified DK1 that considers the major planned upcoming wind power plants and LCC-HVDC links, as shown in Fig. 3. The system contains LCC-HVDC links, doubly-fed induction generator (DFIG) based and permanent magnet synchronous generator (PMSG) based offshore wind farms (OFWFs), an aggregated onshore wind farm (ONWF), and three SCs (SCs 1-3) distributed at the major LCC-HVDC terminals [27]. The other three SCs (SCs 4-6) are installed to support inertial response, reactive power, and short-circuit pow-

er as the system is operated without local synchronous generators. Three OFWFs are Anholt (AHA 400 MW), Horns Rev I (HRA 169 MW), and Horns Rev II and III (HRB 200 MW and HRC 400 MW). The system is synchronized with the German grid, which is modeled by a simplified synchronous machine with a low-inertia constant. An oscillation is found after a frequency disturbance, as shown in Fig. 4.

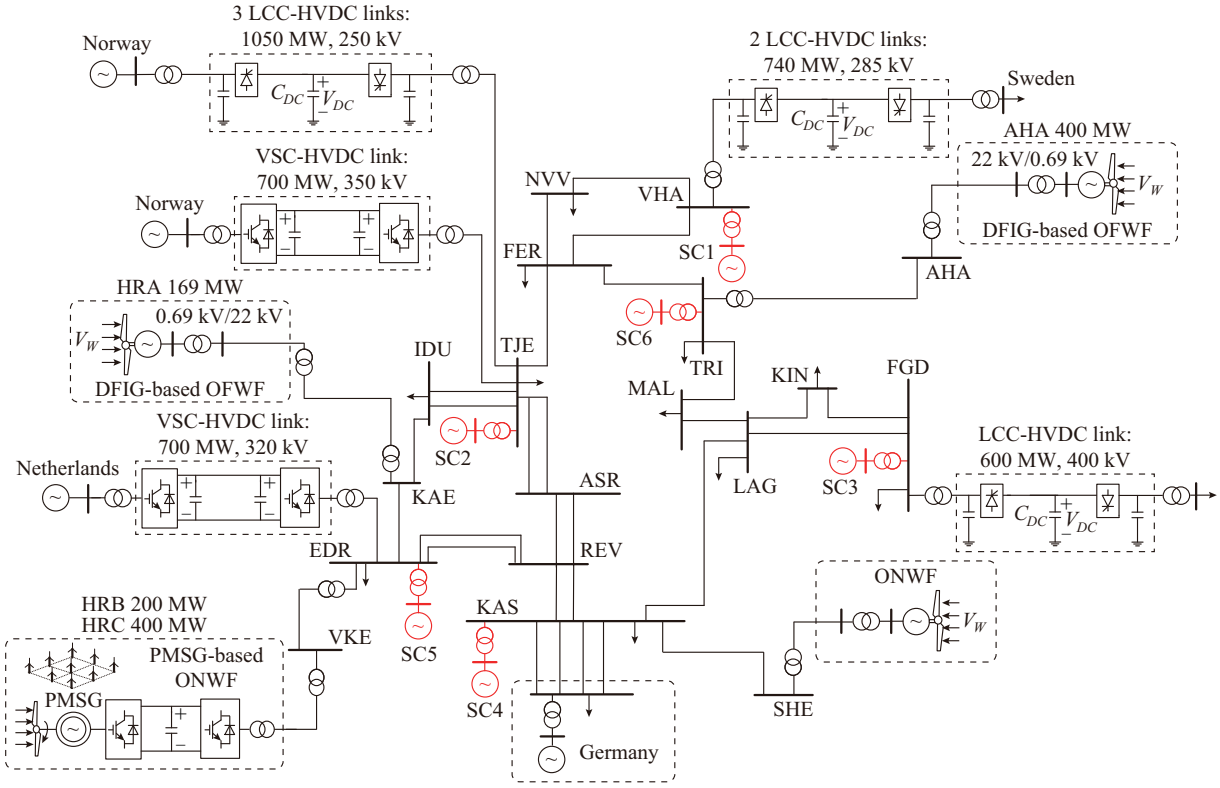

Fig. 3. Single-line diagram of a 400 kV renewable-based DK1 in 2020.

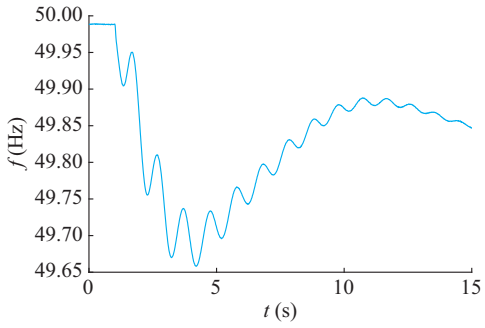

Fig. 4. Power oscillation in prospective future DK1.

The oscillation verified by a sensitivity study takes place between the external grid and the major converter stations instead of using synchronous machines only, which in this case are SCs. To illustrate the contributions of different components to the oscillation, Fig. 5 shows two scenarios investigated in the whole DK1. It can be seen that without the major wind power plant, the post-contingency oscillation of the frequency response is highly reduced and rapidly damped. Meanwhile, the oscillation effect without an SC is only on the phase delay. It can be envisaged that by replacing synchronous machines with more power converters in a power system, the converters will become the main oscillation sources. Owing to the complexity of the inertia characteristics of a low-inertia system, the oscillation mode may shift over time depending on the online generator types and the performance of converter control systems. This requires innovative solutions for an oscillation damping controller that adapts to the modern system characteristics to guarantee a secure operation.

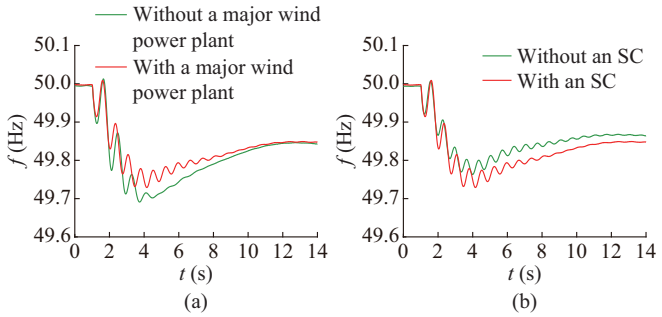

Fig. 5. Sensitivities of different components of oscillation in whole DK1. (a) Frequency response of whole DK1 with and without a major wind power plant. (b) Frequency response of whole DK1 with and without an SC.

To verify the performance of the proposed POD controller on the damping and frequency stability, a load increase scenario and a three-phase short-circuit fault scenario are investigated. To determine how the PSS performs in low-inertia systems, a comparison of system responses with the PSS that is tuned well in [22], with the proposed POD controller

and without either of them (denoted as WO) is investigated in the first scenario. It is worth noting that the modeled future DK1 system is a low-inertia system owing to the high penetration of non-synchronous units, LCC-HVDC links, and a weak German grid. The Danish power system is divided into two non-synchronous areas: the DK1 is synchronized with the continental European system, whereas the eastern Danish power system (denoted as DK2) is synchronized with the Nordic power system, which includes Sweden, Norway, and Finland. DK1 and DK2 are linked by an LCC-HVDC link, which is known as the Great Belt Power Link with a transmission capacity of 600 MW at 400 kV DC. In Fig. 3, all synchronous generators are phased out and six SCs are installed. Meanwhile, the SCs at buses FGD and KAS (SC3 and SC4) are equipped with the proposed POD controller.

A. Load Increasing Scenario

Figure 6 shows the comparative results in load increasing scenario. As shown in Fig. 6(a), in the WO case, a large and long oscillation (the dominant oscillation mode has a 0.079 damping ratio) and a significant frequency deviation (0.3 Hz) are experienced before obtaining a new equilibrium. By contrast, with the proposed POD controller, these parameters are remarkably improved by a damping ratio of 0.29 and a frequency deviation of 0.18 Hz. Consequently, the system response is significantly enhanced. Meanwhile, as shown in Fig. 6(b), with the proposed POD controller, the faster damping and quicker settling down of the ROCOF are realized.

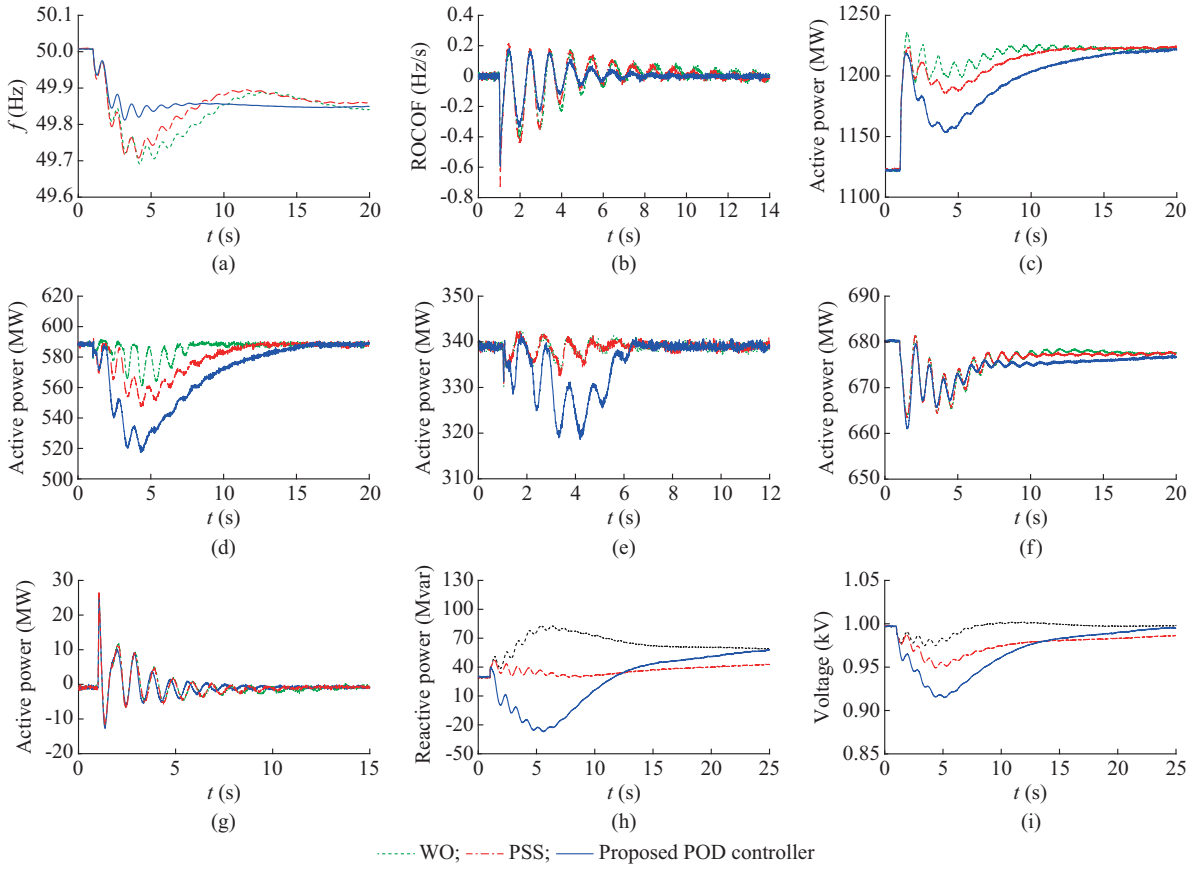

Fig. 6. Comparative results in load increasing scenario. (a) Frequency. (b) ROCOF. (c) Active power from bus KAS to bus LAG. (d) Active power of LCC-HVDC link from DK1 to DK2. (e) Active power of a load. (f) Active power of VSC-HVDC link from DK1 to Holland. (g) Active power of SC. (h) Reactive power of SC. (i) Terminal voltage of SC.

Since the active power shown in Fig. 6(c) - (f) are controlled with the proposed POD controller during the disturbance to reduce the power imbalance and damp the oscillation, the system frequency with the proposed POD controller is improved in terms of the oscillation damping, frequency nadir, and settling time, as shown in Fig. 6(a).

An opposite trend is observed from the reactive power response of the SC during the disturbance without and with the proposed POD controller. Instead of rapidly increasing the reactive power from 31 Mvar to approximately 83 Mvar to keep the voltage constant at the nominal value as in the WO case, the proposed POD controller decreases the terminal voltage by absorbing approximately 58 Mvar reactive power (from 31 Mvar to approximately −27 Mvar) to control the power flow. Consequently, a larger decrease and less oscillation are seen from the active power curves shown in Fig. 6(c)-(e).

As expected, the SC rapidly releases kinetic energy for the inertial response and quickly settles down with the proposed POD controller, as shown in Fig. 6(g). Consequently, the power oscillation and frequency stability are improved during the disturbance with the proposed POD controller.

The comparison of the dominant oscillation mode information in 3 cases is listed in Table II, which shows a significant enhancement in terms of the frequency stability and power oscillation with the proposed POD controller.

TABLE II
COMPARISON OF DOMINANT OSCILLATION MODE IN THREE CASES

Case	Dominant mode	Frequency (Hz)	Damping ratio	Frequency nadir (Hz)	Settling time (s)
WO	−0.525± j6.585	1.048	0.079	49.70	~17
PSS	−0.635± j6.870	1.093	0.092	49.71	~16
Proposed POD controller	−1.933± j6.379	1.015	0.290	49.82	~8

To clarify the active power decrease in the LCC-HVDC link, the rectifier is set to maintain the DC current at its set-point by controlling the firing angle. When the busbar voltage decreases, the DC current is less than its set-point, and the rectifier tends to reduce the firing angle, hence increasing the DC current. However, the firing angle reduction hits the minimum firing angle limit (typically 5°). This results in a decrease in DC current, thereby reducing the active power of LCC-HVDC during the disturbance.

By comparison, the PSS does not operate well in the converter-based system, while the proposed POD controller can further improve the frequency stability and damping ratio by absorbing more reactive power to allow for a lower voltage that still satisfies the grid code.

B. Three-phase Short-circuit Fault Scenario

The proposed POD controller is verified through a severe disturbance with a three-phase short-circuit fault and a load trip occurring simultaneously. A three-phase short-circuit fault is applied on one of the feeders of the bus TRI at t = 1 s, and is cleared at t = 1.1 s. Then, the circuit breaker of the feeder suddenly disconnects the load (250 MW). The comparison of the system responses with and without the proposed POD controller is shown in Fig. 7. The system without the proposed POD controller exhibits a severe oscillation and collapse after approximately 4 s, while the system with the proposed POD controller performs better damping and becomes stable after the fault.

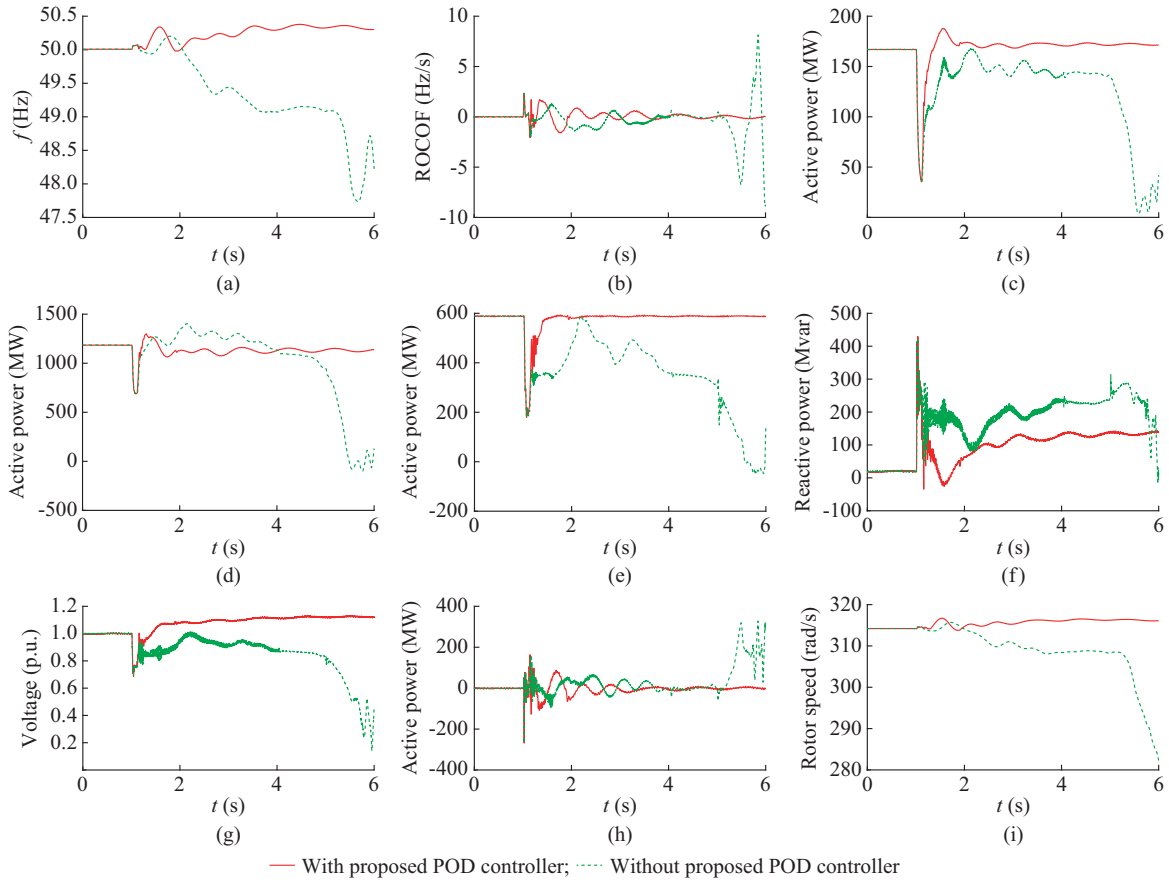

Fig. 7. Comparative results in three-phase short-circuit fault scenario with and without proposed POD controller. (a) System frequency. (b) ROCOF. (c) Active power of load at bus FER. (d) Active power from bus KAS to bus LAG. (e) Active power from DK1 to DK2 through HVDC connection. (f) Reactive power of SC. (g) Terminal voltage of SC. (h) Active power of SC. (i) Rotor speed of SC.

As shown in Fig. 8, for the scenario without the proposed POD controller, the frequencies at different substations (FGD, TJE, and KAS) tend to oscillate against each other after the fault, which leads to a system collapse, while they quickly become stable with the proposed POD controller. Because of the asynchronism issue, the active power could not transfer from Germany to the DK2, as shown in Fig. 7(d)-(e).

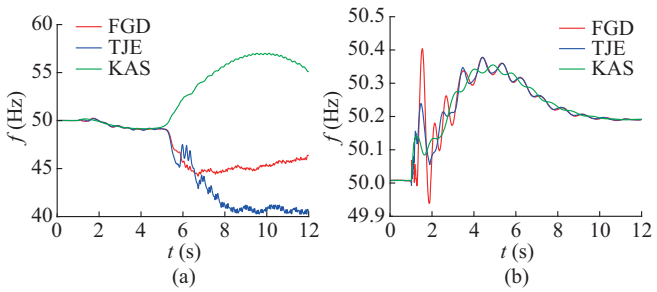

Fig. 8. Frequency responses at different substations during a three-phase short-circuit fault. (a) Without proposed POD controller. (b) With proposed POD controller.

Instead of decreasing the reactive power to prevent the voltage surge, the proposed POD controller allows the terminal voltage to increase within the limit range. Therefore, the transmission line, LCC-HVDC link, and load can absorb more active power to offset the power imbalance during the load trip, as shown in Fig. 7(c)-(e). This phenomenon helps the system maintain stability after the fault.

In this scenario, the active power of the LCC-HVDC link does not contribute significantly to the power oscillation control during the disturbance with the proposed POD controller. It can be explained that the busbar voltage increases, making the DC current higher than the current setpoint. With the ability of firing angle control to transiently reach 90° in order to quickly reduce the DC current, the active power can be kept constant during the voltage increase. By contrast, the load tends to absorb more active power to counteract the power imbalance and damp the oscillation, as shown in Fig. 7(c).

V. Conclusion

To deal with the faster frequency dynamic and oscillatory stability issues in modern power systems that introduce new stability issues and requirements for the controls, this study uses a POD controller incorporating SC by controlling the terminal voltage through the reactive power regulation to improve the frequency dynamic and damp the power oscillations for low-inertia systems. The Prony technique is applied to extract the system oscillation characteristics from the measurement data, which benefits large-scale systems with thousands of variables. The optimization of the POD parameters with a damping ratio maximization objective is implemented by the SiL simulation. Comparative results show that by controlling the terminal voltage, the POD and frequency stability can be significantly improved by SC with the POD controller. In addition, the parameter optimization algorithm can help controller designers, thereby saving time while still offering near-optimal or optimal solutions for the control parameter set compared with the empirical tuning method.

To properly apply the POD controller to a specific power grid, some conclusions are drawn as follows.

1) Controlling the terminal voltage of the SC to change the active power should consider the limitation of transmission lines, LCC-HVDC links, and loads so as to set the limit values for the output of the POD controller.

2) The limits of the terminal voltage of the connected busbar may impact the components connected to the same bus of the SC (PV system, wind generator), which are sensitive to the low-voltage ride-through threshold, voltage-based protection, etc.

3) The transmission line selected for controller design should represent the paths for major oscillations in a network.

References

[1] H. Abildgaard and N. Qin, "Synchronous condensers for reliable HVDC operation and bulk power transfer," in *Proceedings of IEEE 2015 PES General Meeting*, Denver, USA, Jul. 2015, pp. 1-9.

[2] T. van Cutsem and R. Mailhot, "Validation of a fast voltage stability analysis method on the Hydro-Quebec system," *IEEE Transactions on Power Systems*, vol. 12, no. 1, pp. 282-292, Feb. 1997.

[3] I. Kamwa, J. Beland, G. Trudel *et al*., "Wide-area monitoring and control at Hydro-Quebec: past, present and future," in *Proceedings of 2006 IEEE PES General Meeting*, Montreal, Canada, Jun. 2006, pp. 1-12.

[4] P. E. Marken, J. P. Skliutas, P. Y. Sung *et al*., "New synchronous condensers for Jeju island," in *Proceedings of 2012 IEEE PES General Meeting*, San Diego, USA, Jul. 2012, pp. 1-6.

[5] J. W. Park, Y. H. Park, and S. I. Moon, "Instantaneous wind power penetration in Jeju island," in *Proceedings of 2008 IEEE PES General Meeting*, Pittsburgh, USA, Jul. 2008, pp. 1-7.

[6] P. E. Marken, M. Henderson, D. LaForest *et al*., "Selection of synchronous condenser technology for the Granite substation," in *Proceedings of IEEE PES T&D 2010*, New Orleans, USA, Apr. 2010, pp. 1-6.

[7] J. Skliutas, D. LaForest, R. D'Aquila *et al*., "Next-generation synchronous condenser installation at the VELCO granite substation," in *Proceedings of 2009 IEEE PES General Meeting*, Calgary, Canada, Jul. 2009, pp. 1-8.

[8] H. T. Nguyen, G. Cesar, G. Yang *et al*., "Talega SynCon – power grid support for renewable-based systems," in *Proceedings of 2018 Western Protective Relay Conference*, Spokane, USA, Oct. 2018, pp. 1-5.

[9] J. P. Skliutas, R. D. Aquila, J. M. Fogarty *et al*., "Planning the future grid with synchronous condensers," in *Proceedings of CIGRE US National Committee 2013 Grid of the Future Symposium*, Boston, USA, Oct. 2013, pp. 1-11.

[10] M. Nedd, C. Booth, and K. Bell, "Potential solutions to the challenges of low inertia power systems with a case study concerning synchronous condensers," in *Proceedings of 2017 52nd International Universities Power Engineering Conference (UPEC)*, Heraklion, Greece, Aug. 2017, pp. 1-6.

[11] H. Zhang, J. P. Hasler, N. Johansson *et al*., "Frequency response improvement with synchronous condenser and power electronics converters," in *Proceedings of 2017 IEEE 3rd International Future Energy Electronics Conference and ECCE Asia*, Kaohsiung, China, Jun. 2017. pp. 1002-1007.

[12] N. A. Masood, R. Yan, T. K. Saha *et al*., "Frequency response and its enhancement using synchronous condensers in presence of high wind penetration," in *Proceedings of 2015 IEEE PES General Meeting*, Denver, USA, Jul. 2015, pp. 1-5.

[13] A. Moeini and I. Kamwa, "Analytical concepts for reactive power based primary frequency control in power systems," *IEEE Transactions on Power Systems*, vol. 31, no. 6, pp. 4217-4230, Nov. 2016.

[14] Z. Obaid, L. Cipcigan, L. Abrahim *et al*., "Frequency control of future power systems: reviewing and evaluating challenges and new control methods," *Journal of Modern Power Systems and Clean Energy*, vol. 7, no. 1, pp. 9-25, Jan. 2019.

[15] S. Essallah, A. Bouallegue, and A. Khedher, "Integration of automatic voltage regulator and power system stabilizer: small-signal stability in DFIG-based wind farms," *Journal of Modern Power Systems and Clean Energy*, vol. 7, no. 5, pp. 1115-1128, Sept. 2019.

[16] Y. Katsuya, Y. Mitani, and K. Tsuji, "Power system stabilization by synchronous condenser with fast excitation control," in *Proceedings of 2000 International Conference on Power System Technology*, Perth, Australia, Dec. 2000, pp. 1563-1568.

[17] H. T. Nguyen, G. Yang, A. H. Nielsen *et al*., "Hardware and software-in-the-loop simulation for parameterizing the model and control of synchronous condensers," *IEEE Transactions on Sustainable Energy*, vol. 10, no. 3, pp. 1593-1602, Jul. 2019.

[18] W. W. Price, C. W. Taylor, and G. J. Rogers, "Standard load models for power flow and dynamic performance simulation," *IEEE Transactions on Power Systems*, vol. 10, no. 3, pp. 1302-1313, Aug. 1995.
[19] Y. Chen, "Replacing a PID controller by a lag-lead compensator for a robot – a frequency response approach," *IEEE Transactions on Robotics and Automation*, vol. 5, no. 2, pp. 174-182, Apr. 1989.
[20] P. Kundur, *Power System Stability and Control*. New York: McGraw-Hill, 1994.
[21] A. Murdoch, S. Venkataraman, R. A. Lawson *et al*., "Integral of accelerating power type PSS I: theory, design, and tuning methodology," *IEEE Transactions on Energy Conversion*, vol. 14, no. 4, pp. 1658-1663, Dec. 1999.
[22] I. Kamwa, R. Grondin, and G. Trudel, "IEEE PSS2B versus PSS4B: the limits of performance of modern power system stabilizers," *IEEE Transactions on Power Systems*, vol. 20, no. 2, pp. 903-915, May 2005.
[23] L. H. Hassan, M. Moghavvemi, H. A. F. Almurib *et al*., "A coordinated design of PSSs and UPFC-based stabilizer using genetic algorithm," *IEEE Transactions on Industry Applications*, vol. 50, no. 5, pp. 2957-2966, Sept. 2014.
[24] W. M. D. Rosa, P. Rossoni, J. C. Teixeira *et al*., "Optimal allocation of capacitor banks using genetic algorithm and sensitivity analysis," *IEEE Latin America Transactions*, vol. 14, no. 8, pp. 3702-3707, Aug. 2016.
[25] L. Scharf, *Statistical Signal Processing: Detection, Estimation, and Time Series Analysis*. New York: Addison-Wesley, 1991.
[26] X. Xia, C. Li, and W. Ni, "Dominant low-frequency oscillation modes tracking and parameter optimisation of electrical power system using modified Prony method," *IET Generation, Transmission & Distribution*, vol. 11, no. 17, pp. 4358-4364, Nov. 2017.
[27] H. T. Nguyen, G. Y. Yang, A. H. Nielsen *et al*., "Combination of synchronous condenser and synthetic inertia for frequency stability enhancement in low-inertia systems," *IEEE Transactions on Sustainable Energy*, vol. 10, no. 3, pp. 997-1005, Jul. 2019.

Ha Thi Nguyen received the B. Sc., M. Sc., and Ph. D. degrees in electric power systems from University of Science and Technology – the University of Danang, Danang, Vietnam, in 2010, National Cheng Kung University, Tainan, China, in 2014, and Technical University of Denmark (DTU), Lyngby, Denmark, in 2018, respectively. In 2017, she was a Visiting Scholar at the Center Energy Research, University of California San Diego, San Diego, USA. Currently, she is working as a Postdoc at the Center for Electric Power and Energy at DTU. Her research interests include power system operation and control, frequency stability and control, renewable energy integration, real-time co-simulation, and distributed power hardware-in-the-loop simulation.

Guangya Yang received the Ph. D. degree in 2008 from the University of Queensland, Queensland, Australia, in the field of electrical power systems. Currently, he is Senior Power System Engineer with Ørsted and Senior Scientist with Technical University of Denmark, Lyngby, Denmark. Since 2009, he has been developing and leading many industrial collaborative projects in Denmark. He is an Editorial Board Member of IEEE Transactions on Sustainable Energy, IEEE Transactions on Power Delivery, IEEE Access, and Journal of Modern Power Systems and Clean Energy. His research experiences range from power system security, offshore wind power system design and control, and transactive energy applied to integrate distributed energy resources. His research focus is currently on the low-inertia system stability and control with respect to the integration of offshore wind power systems.

Arne Hejde Nielsen is an Associate Professor at the Centre for Electric Power and Energy, Department of Electrical Engineering, Technical University of Denmark, Lyngby, Denmark. He has 30-year experiences in electric power engineering; the first years were from ASEA AB, Central Research and Development Department, Sweden, with focus on measurement technology and motor design and control. Over the past decade, his focus has been on electric power systems, especially on the implementation of renewable energy sources in the power system.

Peter Højgaard Jensen received the M. Sc. degree in electrical engineering from the Technical University of Denmark, Lyngby, Denmark, in 1979. Currently, he is a System Specialist at Siemens A/S. He has 34-year experiences from Danish Power Plants in maintenance, operation, management, engineering, power plant erection and commissioning. Five years in Siemens have been used for developing new control concept for synchronous condensers and commissioning of 13 synchronous condensers (175-270 Mvar) in Denmark, Norway, and USA.

Bikash Pal received B. E. E. degree (with honors) from Jadavpur University, Calcutta, India, the M. E. degree from the Indian Institute of Science, Bangalore, India, and the Ph. D. degree from Imperial College London, London, UK, in 1990, 1992, and 1999, respectively, all in electrical engineering. Currently, he is a Professor in the Department of Electrical and Electronic Engineering, Imperial College London. He is Vice President Publications, IEEE Power & Energy Society. He was Editor-in-Chief of IEEE Transactions on Sustainable Energy (2012-2017) and Editor-in-Chief of IET Generation, Transmission and Distribution (2005-2012) and is a Fellow of IEEE for his contribution to power system stability and control. His current research interests include renewable energy modelling and control, state estimation, and power system dynamics.